

Protein and Virus Crystal Growth on International Microgravity Laboratory-2

Stanley Koszelak, John Day, Cathy Leja, Robert Cudney, and Alexander McPherson
Department of Biochemistry, University of California, Riverside, Riverside, California 92521 USA

ABSTRACT Two $T = 1$ and one $T = 3$ plant viruses, along with a protein, were crystallized in microgravity during the International Microgravity Laboratory-2 (IML-2) mission in July of 1994. The method used was liquid-liquid diffusion in the European Space Agency's Advanced Protein Crystallization Facility (APCF). Distinctive alterations in the habits of Turnip Yellow Mosaic Virus (TYMV) crystals and hexagonal canavalin crystals were observed. Crystals of cubic Satellite Tobacco Mosaic Virus (STMV) more than 30 times the volume of crystals grown in the laboratory were produced in microgravity. X-ray diffraction analysis demonstrated that both crystal forms of canavalin and the cubic STMV crystals diffracted to significantly higher resolution and had superior diffraction properties as judged by relative Wilson plots. It is postulated that the establishment of quasi-stable depletion zones around crystals growing in microgravity are responsible for self-regulated and more ordered growth.

INTRODUCTION

Macromolecular crystal growth has assumed an important place in modern biochemistry and molecular biology because it is pivotal to the development of new structural information based on x-ray diffraction analysis (McPherson, 1989, 1990). One intriguing area of research in this regard has been attempts to grow macromolecular crystals in space, in a totally quiescent and gravity-free environment.

The underlying hypothesis of this approach is that the absence of gravity will eliminate sedimentation and, of even greater importance, that the transport mechanisms responsible for the delivery of molecules from solution to the growing crystal face will be altered markedly. This latter effect is manifested as a transition from convective transport processes that dominate solution transport in the presence of gravity to a wholly diffusive transport regime found in microgravity (Pusey and Naumann, 1986). The kinetics of growth, incorporation of impurities, and many other features of crystal growth are dependent on transport phenomena. Thus, microgravity crystals are expected to show some differences when compared with equivalent crystals grown on earth. Classical theories of crystal growth of conventional materials predict that the absence of gravity would produce positive, rather than negative, effects on the quality of crystals. Thus, growth of macromolecular crystals in microgravity might provide a way to improve the diffraction properties, size, or morphology of protein, nucleic acid, and virus crystals used in x-ray structure analyses.

Experiments on macromolecular crystal growth in microgravity have been carried out now for over 10 years using a

variety of different techniques and instruments, and a number of reports for specific proteins or viruses have been quite favorable and encouraging (DeLucas et al., 1989; Day and McPherson, 1992; Littke, 1988; Littke and John, 1984; Erdmann et al., 1989; McPherson, 1993). In other cases, often not described in the literature, the results have not differed significantly from those seen on earth. A continuing question, therefore, is which kinds or classes of macromolecules and crystals are most likely to benefit from the microgravity experience, and what technical aspects of the process are important for obtaining optimal results. The results reported here are a part of our continuing efforts to answer those questions.

MATERIALS AND METHODS

The experiments described here were carried out in the European Space Agency (ESA) designed Advanced Protein Crystallization Facility (APCF) built by Dornier Aerospace Co. of Friedrichshafen, Germany (for details of design and operation, see Bosch et al., 1992). The method used was direct liquid-liquid diffusion (free interface diffusion (Salemme, 1972) carried out in quartz cells. The volume of all protein chambers was 470 μl , and that of the precipitant chambers was 590 μl . The diffusion cell was activated 3.5 h after a microgravity environment was achieved by 90° rotation of a stopcock that provided continuity between the two chambers through a channel of length 12 mm and volume 235 μl . The cells were deactivated ~12.5 days later by reverse rotation of the stopcocks.

All crystallization cells, 96 in all, were contained within two thermal enclosures maintained at $20.0 \pm 0.1^\circ\text{C}$. For the experiments described here, 15 crystallization cells were available, and they were preloaded with solutions five days before launch as recorded in Table 1. Considerable care was taken to ensure that the presence of bubbles in the chambers was eliminated by repeated topping off and reloading over a 3-day period before handing over the APCF to flight operations personnel.

The experiments were carried out during a Space Shuttle mission of 13 days dedicated solely to microgravity experiments and titled "International Microgravity Laboratory-2." The launch was July 8, 1994 from Kennedy Space Center, Florida, and the landing at the launch site was on July 23, 1994. Unloading of samples took place 4.5 h after landing, and sample examination and photography were carried out immediately. The 15 crystallization cells were returned to the laboratories at the University of California at Riverside in temperature-controlled containers. The cells were

Received for publication 9 January 1995 and in final form 9 March 1995.

Address reprint requests to Dr. Alexander McPherson, Department of Biochemistry, University of California, Room 2466, Boyce Hall, Riverside, CA 92521. Tel.: 909-787-5391; Fax: 909-787-3790; E-mail: mcpherson@ucr.acf.ucr.edu.

© 1995 by the Biophysical Society

0006-3495/95/07/13/07 \$2.00

TABLE 1

Sample	Reactor #	Precipitant connector	Concentration reservoir	Results
TYMV 15 mg/ml	205	0.8 M (NH ₄) ₂ PO ₄	1.0 M (NH ₄) ₂ PO ₄	many large crystals
TYMV 15 mg/ml	207	0.8 M (NH ₄) ₂ PO ₄	1.2 M (NH ₄) ₂ PO ₄	microcrystals
TYMV 15 mg/ml	222	0.8 M (NH ₄) ₂ PO ₄	1.5 M (NH ₄) ₂ PO ₄	many small crystals
SPMV 20 mg/ml	204	12% PEG 8000	12% PEG 8000	microcrystals
SPMV 20 mg/ml	206	15% PEG 8000	15% PEG 8000	microcrystals
STMV 24 mg/ml	223	14% sat'd (NH ₄) ₂ SO ₄	25% sat'd (NH ₄) ₂ SO ₄	6 large crystals
STMV 24 mg/ml	224	14% sat'd (NH ₄) ₂ SO ₄	30% sat'd (NH ₄) ₂ SO ₄	precipitate
STMV 24 mg/ml	227	14% sat'd (NH ₄) ₂ SO ₄	20% sat'd (NH ₄) ₂ SO ₄	several large crystals
Hexagonal Canavalin 22 mg/ml	208	1.5 × DPBS	2.0 × DPBS	15 large crystals
Hexagonal Canavalin 22 mg/ml	210	1.5 × DPBS	2.0 × DPBS	many medium crystals
Rhombohedral Canavalin 16 mg/ml	228	1.5 × DPBS	2.0 × DPBS	many medium crystals
Cytochrome c, 30 mg/ml	201	2.8 M (NH ₄) ₂ SO ₄	2.8 M (NH ₄) ₂ SO ₄	many large needles
Cytochrome c, 30 mg/ml	202	2.8 M (NH ₄) ₂ SO ₄	2.8 M (NH ₄) ₂ SO ₄	many large needles
Cytochrome c, 30 mg/ml	203	2.8 M (NH ₄) ₂ SO ₄	2.5 M (NH ₄) ₂ SO ₄	1 large crystal
Cytochrome c, 30 mg/ml	229	2.8 M (NH ₄) ₂ SO ₄	2.5 M (NH ₄) ₂ SO ₄	microcrystals & small clusters

unloaded as required for further examination, photography, and x-ray diffraction analysis.

In assessing the quality of crystals grown in microgravity, x-ray diffraction results were compared with the best that had been obtained previously for any of the corresponding crystals grown in the conventional laboratory, in fact, those used in the final refinements of the structures (Ko et al., 1993a, b). For both the rhombohedral and hexagonal canavalin crystals and for TYMV crystals, the sizes of earth grown crystals were comparable with or even larger than those grown in microgravity. For cubic STMV, this was not possible, because the microgravity grown crystals were more than an order of magnitude larger than any previously obtained on earth at any time.

Before and during the mission, APCF cells equivalent to those used in the actual space experiment were loaded with identical macromolecule samples and precipitants and parallel experiments were conducted. Liquid-liquid diffusion trials carried out in a 1-g environment, however, suffer many problems that are absent in microgravity. They are, therefore, rather poor controls for the microgravity experiments. For canavalin, TYMV, and STMV, the results obtained on the ground using the APCF cells were markedly inferior to those obtained in the actual space experiment.

The macromolecule samples used in these experiments were prepared for the flight experiments and have the properties described below.

Canavalin

Canavalin (Sumner and Howell, 1936; Smith et al., 1982) is the major storage protein (vicilin) of the Jack Bean (*Canavalia ensiformis*). It is a trimer of three identical $M_r = 47,000$ subunits arranged with exact three-fold symmetry. The structure of the molecule of $M_r = 142,000$ has been solved by x-ray diffraction (Ko et al., 1993), cloned, and expressed in *Escherichia coli* (Ng et al., 1993). The molecule is disk-shaped with a diameter of about 90 Å and a thickness of 45 Å and has a channel of 18-Å diameter through its center. Canavalin can be crystallized in at least four different crystal forms (Spencer and McPherson, 1975). Solutions of canavalin producing both rhombohedral and hexagonal crystal forms were included in these experiments. The rhombohedral crystals are of space group R3 with equivalent hexagonal unit cell dimensions of $a = b = 136$ Å and $c = 75$ Å. The hexagonal form is of space group P6₃ with $a = b = 126$ Å and $c = 51.5$ Å. The crystals can be grown simply by combining a protein solution of 30 mg/ml in water with 2× Dulbecco's phosphate-buffered saline (DPBS) at pH 6.8. The canavalin samples used in these experiments were recrystallized 4 times from DPBS and were homogeneous based on SDS-PAGE.

Satellite Tobacco Mosaic Virus (STMV)

The plant satellite virus STMV (Valverde and Dodds, 1987) has as its master virus Tobacco Mosaic Virus (TMV). STMV is a $T = 1$ icosahedral

virus of 170 Å diameter and $M_r = 1.4 \times 10^6$. There are 60 identical protein units of $M_r = 14,500$ composing its capsid, which contains 1059 bases of genomic single-stranded RNA. The structure of the virus has been solved by x-ray diffraction analysis (Larson et al., 1993). STMV was prepared for these experiments from infected tobacco plants and was recrystallized several times from ammonium sulfate as described previously (Koszulak et al., 1989). SDS-PAGE showed only a single band at the expected value for the STMV coat protein.

STMV crystallizes from a wide range of precipitants and has been the focus of much crystallization research (Malkin et al., 1993; Malkin and McPherson, 1993). It can be crystallized in at least three different unit cells. The orthorhombic form, of space group I222 with $a = 174.3$ Å, $b = 191.8$ Å, $c = 202.5$ Å, and the monoclinic form of space group I2 with $a = 176.2$ Å, $b = 170.1$ Å, $c = 244.9$ Å, and $\beta = 92.8^\circ$ have been crystallized in previous microgravity experiments and investigated by x-ray diffraction (Day and McPherson, 1992). Solutions yielding the cubic crystal form were used in the experiments described here. The unit cell of these crystals has $a = b = c = 257$ Å with space group I23.

Satellite Panicum Mosaic Virus (SPMV)

The second plant satellite virus SPMV (Buzen et al., 1984) has as its master virus Panicum Mosaic Virus (PMV). It too is a $T = 1$ icosahedral virus of $M_r = 1.2 \times 10^6$ and diameter 170 Å having 60 identical protein subunits of $M_r = 14,000$ composing its capsid which, in turn, contains 860 bases of genomic single-stranded RNA (Masuta et al., 1987). It is isolated from infected millet leaves as described in Day et al. (1994) and was recrystallized twice before inclusion in these experiments. The structure of SPMV has been determined by x-ray diffraction analysis (Ban, unpublished data). SPMV can be crystallized in several unit cells including a monoclinic form obtained from 8–15% PEG 8000 at pH 8.2 with a virus concentration of ~20 mg/ml over a period of 3–6 days. SDS-PAGE showed only a single band corresponding to the molecular weight for the SPMV coat protein.

Turnip Yellow Mosaic Virus (TYMV)

One of the most thoroughly and earliest studied virus known is TYMV (Markham and Smith, 1946; Matthews, 1981), isolated for these experiments from infected Chinese cabbage according to (Canady et al., 1995). TYMV is a $T = 3$ plant virus of $M_r = 5.6 \times 10^6$ and diameter 280 Å, having a capsid composed of 180 identical protein subunits of $M_r = 20,133$. The genome is 1.9 kB of a single strand of RNA. The determination of the structure by x-ray diffraction analysis is currently underway (Canady et al., 1995).

TYMV can be crystallized by combining 15 mg/ml solutions of the purified virus with 0.8–1.5 M ammonium phosphate at pH 3.9. The hexagonal bipyramid crystals are of space group P6₂22 with $a = b = 540$

Å and $c = 320$ Å. They are grown at room temperature over a period of 2–5 days. In the microgravity experiments, $2\times$ recrystallized TYMV was used. These samples exhibited only a single band on SDS-PAGE corresponding to the coat protein molecular weight.

Before loading the samples into the APCF cells, conditions for crystal growth were optimized using liquid-liquid diffusion methods in APCF laboratory cells. It must be recalled, however, that the liquid-liquid diffusion process, because of convection, is quite different in earth's gravity than in space. Thus, there was no way to know with certainty that the optimal earth conditions would transport well to a microgravity environment. Samples were concentrated and sterilized by passage through 0.22- μm filters before loading. Loading was carried out in a flow hood, and clean but not sterile procedures were used.

X-ray diffraction data were collected at 17°C as described previously (Ko et al., 1993a, b; Larson et al., 1993) from capillary-mounted crystals grown on earth and in microgravity using a San Diego Multiwire Systems (SDMS) double-detector multiwire detector system (Xuong et al., 1985) with crystal-to-detector distances of 535 mm for both canavalin crystal forms and 930–985 mm for the cubic STMV crystals. Frame sizes were 0.14° with 2–3 min/frame. The x rays were generated by a Rigaku RU-200 rotating anode generator operated at 45 kV and 145 mA with a Supper monochromator to give 1.54 Å radiation. Crystals were exposed for 24–48 h. The data collection procedures and experimental parameters were identical for both earth- and space-grown crystals. Redundancy of recordings ranged from four to eight. Data correction, reduction, merging, and statistical analysis used the programs supplied by SDMS. For both earth- and microgravity-grown crystals the R_{sym} 's varied from 0.035 to 0.06 to the limits of resolution of the data sets, being somewhat higher for the cubic STMV crystals than for the canavalin crystals.

It should be noted here that the other 77 crystallization cells were used by other investigators from the US and Europe. No attempt will be made to describe their experiments or results because, indeed, they are largely unknown to us at this time.

RESULTS

Canavalin

Both rhombohedral and hexagonal crystals of large size (edges >1 mm in length) were grown in large numbers (on the order of 100) in cells 208, 210, and 228 (see Table 1). Generally, both rhombohedral and hexagonal crystals were seen together, coexisting in the same cells. This is unusual in the laboratory, but not unheard of. It was not seen in any of the control or optimization experiments conducted on earth with the identical protein samples.

Both the rhombohedral and hexagonal crystals were of uniformly high visual quality, as seen in Fig. 1, A and B. The definition of edges was particularly striking for the hexagonal crystals, and both forms were generally free of obvious defects, cracks, macrosteps, striations, or other imperfections. This is consistent with what we reported for canavalin crystals in previous microgravity experiments (McPherson et al., 1991), an increase in visual perfection. The size distribution was excellent, with many large crystals, but none were of exceptional size that exceeded the largest obtained over the past 20 years in the laboratory.

A striking morphological difference between hexagonal canavalin crystals grown in microgravity and on earth was obvious, however. This was the extraordinary cusp, or occlusion, seen along the central prismatic axis of these crystals and shown in detail in Fig. 2 A. The long, deep central

cusp seen in this example was uniformly present in almost all of the hexagonal canavalin crystals grown on the IML-2 mission. Although such hexagonal crystals grown in the laboratory generally show such a cusp when of very small size, these normally fill in during the later stages of growth and ultimately appear like those in Fig. 2 B. This clearly was not the case for the hexagonal canavalin crystals grown in space like that one seen in Fig. 2 A. Interestingly, in our report of the results for canavalin crystallization on IML-1 2 years ago (Day and McPherson, 1992; McPherson, 1993), some comparable observations regarding the shape and size of this central cavity in microcrystals of the hexagonal form were also made.

X-ray diffraction analysis of the microgravity-grown canavalin crystals, both the rhombohedral and the hexagonal form, were both surprising and encouraging. Previously, we had grown canavalin crystals in space on numerous missions using a vapor diffusion technique (DeLucas et al., 1986, 1991). Large rhombohedral crystals frequently were grown in these experiments. When analyzed by x-ray diffraction, they demonstrated a significant improvement in signal-to-noise over the entire resolution range, but no clear improvement in the ultimate resolution of the diffraction pattern (McPherson et al., 1991).

The results from IML-2, however, were quite different, and these are seen in Figs. 3 and 4. Comparative Wilson plots (Wilson, 1949, 1970) of intensity (I/σ) vs. $\sin^2 \theta/\lambda^2$ for six rhombohedral crystals chosen at random from the many grown in the APCF on IML-2 demonstrated a marked improvement compared with the best data we had in hand from earth-grown crystals, indeed, that which we used to actually refine the structure of rhombohedral canavalin (Ko et al., 1993b). Even more striking, an appreciable extension of the resolution of the diffraction pattern was clearly evident for the crystals grown in microgravity.

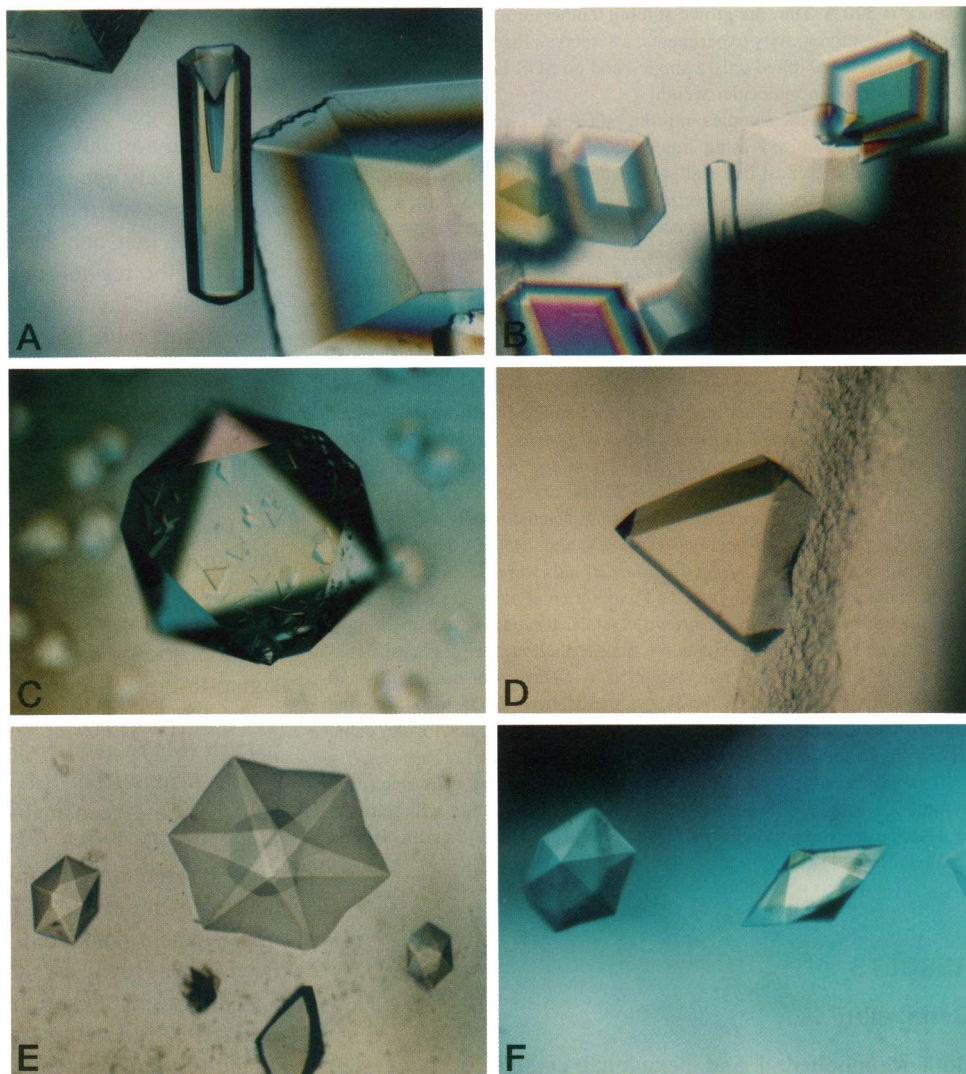
Very similar results were obtained from six crystals of the hexagonal crystal form of canavalin as seen in Fig. 4. Again, there was a substantial improvement in the I/σ ratio over the entire resolution range, and a clear extension of the maximum resolution to a higher value.

For the rhombohedral crystals of canavalin the effective maximum resolution of the available x-ray data was extended from a marginal 2.6 Å (Ko et al., 1993a, b) to at least 2.3 Å Bragg spacings. For the hexagonal crystal form, the extension was from ~ 2.7 Å to nearly 2.2 Å resolution. In the first case, this corresponds to an increase of useful data from 10,127 to 22,561 (Ko et al., 1993b) unique reflections, whereas for the hexagonal case an increase in data from 10,117 to 20,063 (Ko et al., 1993a) reflections. In both cases, this represents a remarkable doubling of useful x-ray data.

STMV

The cubic crystal form of STMV generally grows to limited size in the laboratory, seldom if ever exceeding 0.4 mm on

FIGURE 1 Crystals of proteins and viruses grown by liquid-liquid diffusion on IML-2. In *A* and *B* are seen both rhombohedral and hexagonal crystals of the plant seed protein canavalin. The rhombohedral crystals are up to 1 mm on an edge, as are the lengths of the hexagonal prisms. The latter are characterized by a deep occlusion along the central axis not seen in crystals grown in a conventional laboratory. In *C* and *D* are two examples of the unusually large cubic crystals of STMV, more than 30 times the size of similar crystals grown on earth. The STMV crystal in *D* can be seen nucleated from the surface of the quartz cell. The background of microcrystals seen in *C* are believed to have appeared after re-entry from space. In *E* are crystals of TYMV displaying the unique, multifaceted forms observed only in these microgravity grown crystals. In *F* are seen additional hexagonal bipyramidal crystals of TYMV in the APCF cell. The magnification of all photos is $\times 40$.



an edge, and diffracts to only a low resolution of 6–8 Å. This is in striking contrast to the orthorhombic and monoclinic forms, which grow very large and diffract to 2.3-Å resolution in the laboratory.

Upon removing the crystallization cells from the APCF for photography, we immediately noticed, without visual aids, the extraordinarily large, octahedral habit, cubic crystals growing in cells 223 and 227. All had nucleated on the faces or in the edges and corners of the crystallization cells and, in all, there were ~ 15 of these crystals. The crystals, two of which are shown in Fig. 1, *C* and *D*, had maximum linear dimensions >1.5 mm and were, in the best cases, >30 times the volume of the largest cubic STMV crystals grown on earth.

The diffraction results for three crystals grown in microgravity are shown in Fig. 5. Whether from size alone, or from some enhancement of the internal order, it is clear that the resolution of the diffraction pattern of these crystals was extended significantly and to a limit of ~ 4 -Å resolution vs. 6-Å resolution for the best earth-grown crystals. In addition,

there is again an improvement of the I/σ ratio over the entire resolution range.

TYMV

Crystals of TYMV, like that shown in Fig. 6 *A*, can be readily grown in the laboratory to sizes >1 mm on an edge. From synchrotron data to 3.2-Å resolution, the structure of this $T = 3$, 280-Å-diameter virus currently is being determined. The immediate observation presented by the APCF-grown TYMV crystals produced in a microgravity environment, like those shown in Fig. 6 *B*, is the remarkable alteration in crystal morphology. Hundreds of TYMV crystals were grown in APCF cells 205 and 222, and virtually all displayed the character seen in Fig. 6 *B*. Note the indentation creasing the center of each triangular face and the subtle scalloping of each edge, leading to a significantly more polygonal, multifaceted shape for the crystals. This is clearly the result of growth limited by diffusive transport at the most active points of unit addition.

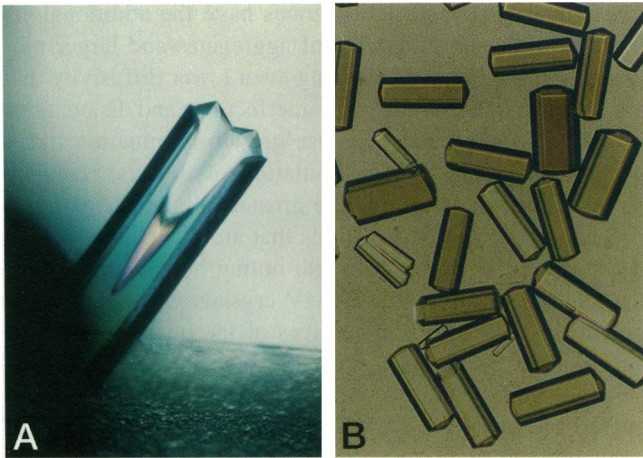


FIGURE 2 In A is a hexagonal crystal of canavalin grown in the APCF during IML-2 displaying the deep cusp along its central axis, a characteristic of nearly all such crystals grown in microgravity. In B are hexagonal canavalin crystals grown in the conventional laboratory, showing the lack of the cusp in fully grown crystals used for diffraction analysis. The magnification of both photographs is $\times 40$.

X-ray diffraction analysis of TYMV crystals could only be carried out in a cursory fashion using our laboratory apparatus because no synchrotron source was available. Using this system, we could not record accurately a representative intensity set over a broad resolution range, and no comparative Wilson plot was possible. We were able, however, to estimate the resolution limit of several crystals but we did not observe, for these crystals, a significant extension of the diffraction pattern.

SPMV

The only crystals observed in the APCF cells for the SPMV samples were very small microcrystals, and only a few of

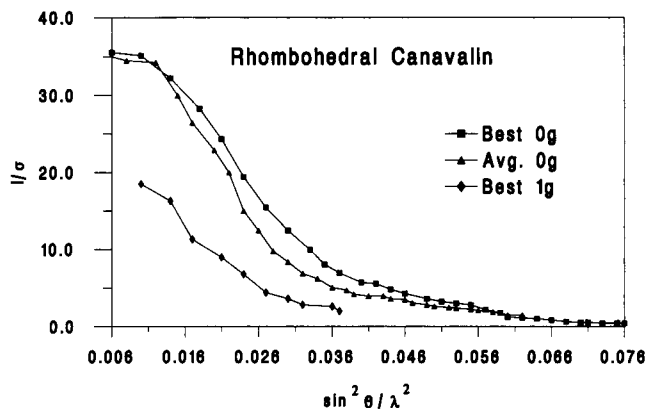


FIGURE 3 A graph of the intensity (I) vs. estimated error (σ) ratio as a function of resolution ($\sin^2 \theta / \lambda^2$) for rhombohedral canavalin crystals grown on earth and in microgravity during IML-2. In this modified Wilson Plot (Wilson, 1949, 1970), the value of I/σ may be taken as the effective "signal-to-noise ratio" for the diffraction pattern at the resolution corresponding to the particular $\sin^2 \theta / \lambda^2$ value. The maximum resolution of the pattern is the point at which the I/σ ratio falls below ~ 1 . Clearly, the "best" microgravity-grown crystal of the six examined, as well as the average of the six, both represent substantial improvements over those crystals grown on earth, which produced the best data previously obtained.

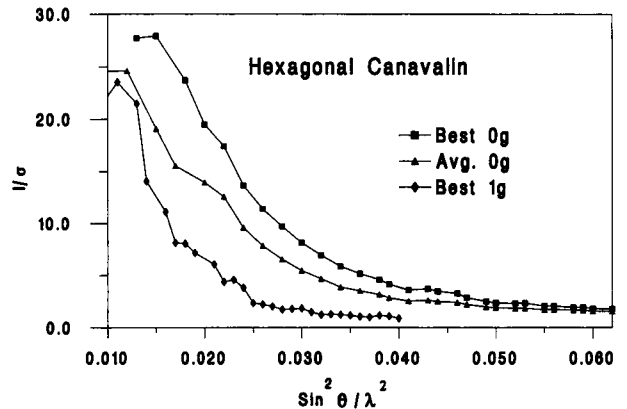


FIGURE 4 The I/σ plot vs. resolution for the "best" of six microgravity-grown hexagonal canavalin crystals, the average of the six, and the best crystals previously available from conventional laboratory investigations. As for the rhombohedral canavalin crystals analyzed in Fig. 3, the microgravity-grown hexagonal crystals clearly demonstrate a higher resolution and improved diffraction properties over the entire resolution range.

them. No meaningful observations or x-ray diffraction data were collected from any of these.

DISCUSSION

There are three kinds of observations or data that emerge from the IML-2 experiments that suggest changes in the phenomenon of macromolecular crystal growth as it occurs in microgravity as compared with that in conventional laboratories. These include alteration in average or maximum size of crystals, morphological modifications, and changes in the diffraction properties.

The most straightforward of these to explain are the morphological changes observed in the canavalin hexagonal crystals and those in the TYMV crystals. Both the deep conical occlusion seen in the former and the scalloping of

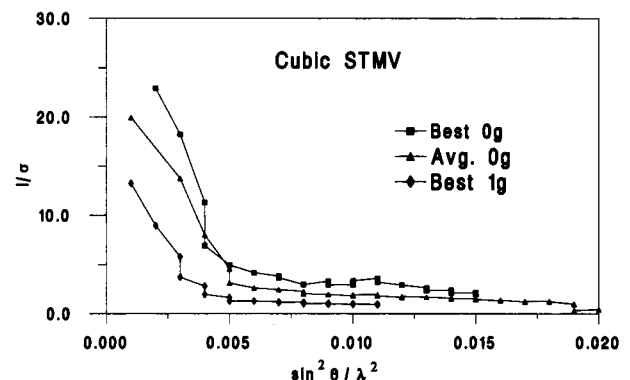


FIGURE 5 The comparative Wilson plot for the "best" of three microgravity-grown cubic STMV crystals from IML-2, the average of the three, and the "best" data previously obtained for crystals grown in the laboratory. As for canavalin, there is a general improvement in the I/σ ratio for all resolution ranges, as well as an extension of the maximum resolution, in this case from ~ 6 to 4 \AA Bragg spacings. The trend seen here is consistent with other microgravity experiments carried out on IML-1 and a variety of other missions.

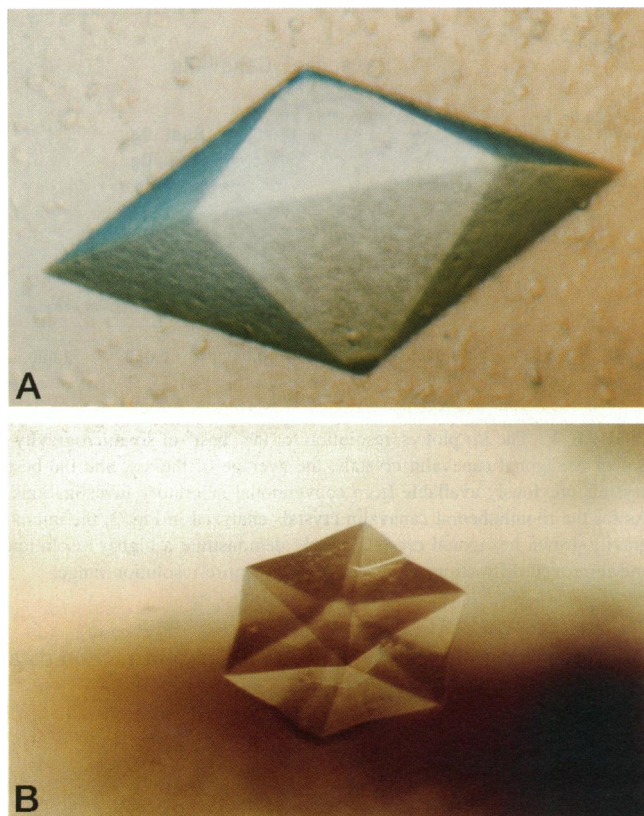


FIGURE 6 In *A* is a typical hexagonal bipyramidal crystal of Turnip Yellow Mosaic Virus (TYMV) grown in the laboratory. The maximum dimension is >1 mm. In *B* are crystals of TYMV grown in microgravity under otherwise similar conditions. The alteration of morphology is striking. In the center of every face is a crease accompanied by a depression in each edge. These are classical signs of diffusion limited growth of the crystals. The magnification of the photo in *A* is $\times 60$, and that in *B* is $\times 40$.

the edges and faces of the latter are readily explained by substitute transfer from the mass transport regime that is dominated by convection on earth to an almost purely diffusive regime that dominates transport in microgravity. Both occur as a consequence of the most rapidly growing points on the crystal creating quasi-stable, local environments of reduced supersaturation leading, in turn, to the retardation of growth at those points. The hexagonal canavalin crystals and the TYMV crystals grown in microgravity, therefore, provide macromolecular versions, and classic examples, of a phenomenon long known and studied for conventional crystals (Chernov, 1984).

The dramatic increase in size observed for the cubic STMV crystals, we believe, is again attributable to diffusive transport processes in the absence of convective mixing. As we have described previously (McPherson, 1993), because of the low diffusivity of macromolecules, and particularly so for viruses because of the large size, regions of reduced supersaturation, or depletion zones, form in the immediate neighborhood of crystals growing in microgravity. This self-regulation of local supersaturation in the neighborhood of growing crystals promotes more ordered and controlled addition of growth units to the developing crystal surfaces.

These quasi-stable depletion zones have the additional effect of limiting the transport of aggregates and larger molecular weight impurities having even lower diffusivity that are the most likely sources of imperfections and dislocations in the growing crystal. Because growth termination likely occurs because of the accumulation of defects, reducing their number tends to promote greater ultimate size.

Some additional observations that are difficult to quantify meaningfully may be worth noting here. Nearly all of the unusually large cubic STMV crystals grown in microgravity had nucleated on surfaces of the quartz cells. This appeared to be a much greater proportion than nucleate heterogeneously in the laboratory. This was not seen, however, for canavalin or TYMV. In Fig. 1 *C*, a large number of cubic microcrystals can be seen in addition to the very large cubic crystals on the quartz surfaces. We suspect that these microcrystals grew after the mission terminated. Very few, if any were seen immediately after the flight, and their number increased after handling the cells during photography. Thus, we believe the very large cubic STMV crystals were the only ones produced in microgravity. This was certainly the case for the very large orthorhombic STMV crystals grown on IML-1 (Day and McPherson, 1992).

We think it worth emphasizing again that a significant improvement in diffraction resolution was obtained for both rhombohedral and hexagonal canavalin crystals using the APCF on IML-2. We have grown rhombohedral canavalin crystals of very large size on a number of previous missions using the vapor diffusion technique (McPherson, 1990) in a device called the Vapor Diffusion Apparatus (VDA; see DeLucas et al., 1986, 1991). In no case, however, did we previously see any significant increase in diffraction resolution. The results we obtained on IML-2, therefore, suggest that the particular technique one uses in microgravity experiments is of substantial consequence.

The failure of SPMV to produce any meaningful crystals is probably attributable to experimental conditions. The SPMV trials were the only liquid-liquid diffusion experiments reported here that used PEG as the precipitating agent. Our impression, shared by other colleagues on this mission who also used PEG in their experiments, is that the diffusion rate of PEG is so slow that only an experiment of very long duration in space, using free interface diffusion, would be successful. Thus, we would predict that optimization of conditions for PEG-based liquid-liquid diffusion will be very difficult to achieve on the ground. Although PEG may be suitable for vapor diffusion and batch crystallization in microgravity, it might be wise to minimize its use in liquid-liquid diffusion trials on flights of relatively short duration until its fluid properties are better understood.

The results we obtained from experiments carried out on IML-2 are consistent with those we conducted on IML-1 and those reported by a number of other investigators from other missions (DeLucas et al., 1989; Day and McPherson, 1992; Littke, 1988; Littke and John, 1984; Erdmann et al., 1989; McPherson, 1993). In a number of cases, some dramatic alterations in crystal morphology were observed,

nearly all explicable in terms of the diffusive transport processes that dominate in microgravity. In addition, some remarkable increases in crystal size were also seen (cubic STMV). Similar results for orthorhombic crystals of STMV were seen from IML-1. Finally, and most encouraging, unequivocal improvements in the quality and resolution of the diffraction patterns for some types of crystals (rhombohedral and hexagonal canavalin, cubic STMV) were clearly evident. Although we cannot readily explain precisely why such improvements were obtained, we again believe them to be a function of the altered kinetics and mechanisms of presentation of molecules to the growing crystal surfaces that exist in microgravity.

The authors thank those NASA and ESA personnel who contributed to the success of these experiments.

This research was supported by a grant from the National Aeronautics and Space Administration.

REFERENCES

- Bosch, R., P. Lautenschlager, L. Potthast, and J. Stapelmann. 1992. Experiment equipment for protein crystallization in μg facilities. *J. Cryst. Growth*. 122:310–316.
- Buzen, F. G., Jr., C. L. Niblett, G. R. Hooper, J. Hubbard, and M. A. Newman. 1984. Further characterization of panicum mosaic virus, and its associated satellite virus. *Phytopathol.* 74:313–318.
- Canady, M. A., J. Day, and A. McPherson. 1995. Preliminary x-ray diffraction analysis of crystals of Turnip Yellow Mosaic Virus (TYMV) *Proteins*. 21:78–81.
- Chernov, A. A. 1984. *Modern Crystallography III*. Springer-Verlag, New York. 208–245.
- Day, J., and A. McPherson. 1992. Macromolecular crystal growth experiments on International Microgravity Laboratory-1. *Protein Sci.* 1:254–1268.
- Day, J., N. Ban, S. Patel, S. B. Larson, and A. McPherson. 1994. Characterization of crystals of satellite panicum mosaic virus. *J. Mol. Biol.* 238:849–851.
- DeLucas, L. J., C. D. Smith, H. W. Smith, V. K. Senagdi, S. E. Senadhi, S. E. Ealick, C. E. Bugg, D. C. Carter, R. S. Snyder, P. C. Weber, F. R. Salemme, D. H. Ohlendorf, H. M. Einspahr, L. Clancy, M. A. Navia, B. M. McKeever, T. L. Nagabhushan, G. Nelson, Y. S. Babu, A. McPherson, S. Koszelak, D. Stammers, K. Powell, and G. Darby. 1989. Protein crystal growth in microgravity. *Science*. 246:651–654.
- DeLucas, L. J., C. D. Smith, W. Smith, V.-K. Senadhi, S. E. Senadhi, S. E. Ealick, D. C. Carter, R. S. Snyder, P. C. Weber, F. R. Salemme, D. H. Ohlendorf, H. M. Einspahr, L. L. Clancey, M. A. Navia, B. M. McKeever, T. L. Nagabhushan, G. Nelson, A. McPherson, S. Koszelak, G. Taylor, D. Stammers, K. Powell, G. Darby, and C. E. Bugg. 1991. Protein crystal growth results for shuttle flights STS-26, and STS-29. *J. Cryst. Growth*. 110:302–311.
- DeLucas, L. J., F. L. Suddath, R. Snyder, R. Naumann, M. B. Broom, M. Pusey, V. Yost, B. Herren, D. Carter, B. Nelson, E. J. Meehan, A. McPherson, and C. E. Bugg. 1986. Preliminary investigations of protein crystal growth using the space shuttle. *J. Cryst. Growth*. 76:681–693.
- Erdmann, V. A., C. Lippmann, C. Betzel, Z. Dauter, K. Wilson, R. Hilgenfeld, J. Hoven, A. Liesum, W. Saenger, A. Muller-Fahrnow, W. Hinrichs, M. Duvel, G. Schulz, C. W. Muller, H. G. Wittmann, A. Yonath, G. Weber, K. Stegen, and A. Plaas-Link. 1989. Crystallization of proteins under microgravity. *FEBS Lett.* 259:194–198.
- Ko, T.-P., J. D. Ng, and A. McPherson. 1993A. The three dimensional structure of canavalin from jack bean. *Plant Physiol.* 101:729–744.
- Ko, T.-P., J. D. Ng, J. Day, A. Greenwood, and A. McPherson. 1993B. X-ray structure determination of three crystal forms of canavalin by molecular replacement. *Acta Cryst.* D49:478–489.
- Koszelak, S., J. A. Dodds, and A. McPherson. 1989. Preliminary analysis of crystals of Satellite Tobacco Mosaic Virus (STMV). *J. Mol. Biol.* 209:323–326.
- Larson, S. B., S. Koszelak, J. Day, A. Greenwood, J. A. Dodds, and A. McPherson. 1993. The three dimensional structure of satellite tobacco mosaic virus at 2.9 Å resolution. *J. Mol. Biol.* 231:375–391.
- Littke, W. 1988. Protein single crystal growth under microgravity. *J. Cryst. Growth*. 90:344–348.
- Littke, W., and C. John. 1984. Protein single crystal growth under microgravity. *Science*. 225:203.
- Malkin, A. J., J. Cheung, and A. McPherson. 1993. Crystallization of satellite tobacco mosaic virus. I. Nucleation Phenomena. *J. Cryst. Growth*. 126:544–554.
- Malkin, A. J., and A. McPherson. 1993. Crystallization of Satellite Tobacco Mosaic Virus. II. Postnucleation events. *J. Cryst. Growth*. 126:555–564.
- Markham, R., and K. M. Smith. 1946. A new crystalline plant virus. *Nature*. 157:300.
- Masuta, C., D. Zuidema, B. G. Hunter, L. A. Heaton, D. S. Sopher, and A. O. Jackson. 1987. Analysis of the genome of satellite panicum mosaic virus. *Virology*. 159:329–338.
- Matthews, R. E. F. 1981. Portraits of viruses: turnip yellow mosaic virus. *Intervirol.* 15:121–144.
- McPherson, A. 1990. Current approaches to macromolecular crystallization. *Eur. J. Biochem.* 189:1–23.
- McPherson, A. 1989. Macromolecular crystals. *Scientific American*. 260:62–69.
- McPherson, A. 1993. Virus, and protein crystal growth on earth, and in microgravity. *J. Phys. D. Appl. Phys.* 26:1993.
- McPherson, A., A. Greenwood, and J. Day. 1991. The effect of microgravity on protein crystal growth. *Adv. Space Res.* 11:343–356.
- McPherson, A., and R. Spencer. 1975. Preliminary structure analysis of canavalin from Jack bean. *Arch. Biochem. Biophys.* 169:650–661.
- Ng, J. D., T.-P. Ko, and A. McPherson. 1993. Cloning, expression, and crystallization of jack bean canavalin. *Plant Physiol.* 101:713–728.
- Pusey, M., and R. Naumann. 1986. Growth kinetics of tetragonal lysozyme crystals. *J. Cryst. Growth*. 76:593–599.
- Pusey, M., W. K. Witherow, and R. Naumann. 1988. Preliminary investigations into solutal flow about growing tetragonal lysozyme crystals. *J. Cryst. Growth*. 90:105–111.
- Salemme, F. R. 1972. A free interface diffusion technique for the crystallization of proteins for x-ray crystallography. *Arch. Biochem. Biophys.* 151:533–537.
- Smith, S. C., S. Johnson, J. Andrews, and A. McPherson. 1982. Biochemical characterization of canavalin: the major storage protein of Jack Bean. *Plant Physiol.* 70:1199–1208.
- Sumner, J. B., and S. F. Howell. 1936. The isolation of a form of crystallizable jack bean globulin through the digestion of canavalin with trypsin. *J. Biol. Chem.* 113:607–610.
- Valverde, R. A., and J. A. Dodds. 1987. Some properties of isometric virus particles which contain the satellite RNA of tobacco mosaic virus. *J. Gen. Virol.* 68:965–972.
- Wilson, A. J. C. 1949. The probability distribution of x-ray intensities. *Acta Crystallogr.* 2:318–321.
- Wilson, A. J. C. 1970. *Elements of X-Ray Crystallography*. Addison-Wesley, Reading, MA.
- Xuong, N.-H., C. Nielson, R. Hamlin, and D. Anderson. 1985. Strategy for data collection from protein crystals using a multi-wire counter area detector diffractometer. *J. Appl. Crystallogr.* 18:342–360.